Stepwise versus Direct Long-Range Charge Separation in Molecular Triads

R. J. Willemse,[†] J. J. Piet,[‡] J. M. Warman,[‡] F. Hartl,[†] J. W. Verhoeven,[†] and A. M. Brouwer*,[†]

Contribution from the Institute of Molecular Chemistry, University of Amsterdam, Nieuwe Achtergracht 129, 1018 WS Amsterdam, The Netherlands, and IRI, Delft University of Technology, Mekelweg 15, 2629 JB Delft, The Netherlands

Received October 22, 1998. Revised Manuscript Received January 27, 2000

Abstract: Trifunctional electron donor−donor−acceptor molecules are described in which photoinduced charge separation, $D_2-D_1-A^* \rightarrow D_2-D_1^+-A^-$, is followed by a charge migration step $D_2-D_1^+-A^-$ (CS1) $\rightarrow D_2^+-D_1-A^-$ (CS2), leading to a relatively long-lived charge-separated state. The rate of the charge migration process could be determined in a range of solvents of low polarity. In benzene and dioxane, reversibility of the process allowed the determination of the free energy difference between CS1 and CS2. The relative energy of the CS2 state is much lower than expected from simple electrostatic models. An increase of the charge migration rate was found with increasing solvent polarity within a series of alkyl ethers or alkyl acetates. However, an apparent preferential stabilization of the CS1 state in acetates relative to ethers leads to discontinuities in the solvatochromic shift behavior of the CT fluorescence from the CS1 state, and in the increase of the charge migration rate as a function of dielectric constant. In a reference compound lacking the intermediate redox unit, direct long-range charge separation yielding a D_2^+-bridge$-A^-$ charge-separated state can occur, but the yield is significantly lower than in the triads.

Introduction

The process of photoinduced charge separation via a sequence of short-range electron transfer steps as it occurs in natural photosynthesis has inspired many chemists to design molecular systems which may accomplish the same efficient and long-lived charge separation. Some groups have used building blocks that resemble the chromophores of Nature,[1−3] and more or less attempt to mimic the photosynthetic apparatus,[4] while others have implemented multistep charge separation schemes in very differently constructed organic,[5−14] inorganic,[15−17] and supramolecular systems.[18−20]

The overall efficiency in multistep charge separation sequences depends critically on the competition between forward charge separation steps and charge recombination processes. In the "photosynthetic model systems" described in the literature, large variations are found in the overall quantum yields and lifetimes of the ultimate charge-separated state. What we find particularly striking is the large variation in the rates of recombination of the charge-separated states, remarkably rapid recombination being found in some cases even with very substantial distances between the charged sites.[2,9,12,16]

Many of the model systems studied require relatively polar solvents to achieve charge separation, which has the drawback that they usually do not work in immobilized media (in which solvent reorganization is highly restricted) or at (very) low temperatures. Moreover, the use of a polar solvent introduces a large solvent reorganization term which tends to enhance the rate of charge recombination considerably.[9] Thus, being able to separate charges in a medium of low polarity is an attractive

* Author to whom correspondence should be addressed. Fax +31 20 5255670. E-mail: fred@org.chem.uva.nl.

† University of Amsterdam.

‡ Delft University of Technology.

(1) Gust, D.; Moore, T. A.; Moore, A. L. *Acc. Chem. Res.* **1993**, *26*, 198.

(2) Osuka, A.; Marumo, S.; Mataga, N.; Taniguchi, S.; Okada, T.; Yamazaki, I.; Nishimura, Y.; Ohno, T.; Nozaki, K. *J. Am. Chem. Soc.* **1996**, *118*, 155.

(3) Osuka, A.; Mataga, N.; Okada, T. *Pure Appl. Chem.* **1997**, *69*, 797.

(4) Wasielewski, M. R.; Gaines, G. L.; Wiederrecht, G. P.; Svec, W. A.; Niemczyk, M. P. *J. Am. Chem. Soc.* **1993**, *115*, 10442.

(5) Mes, G. F.; van Ramesdonk, H. J.; Verhoeven, J. W. *J. Am. Chem. Soc.* **1984**, *106*, 1335.

(6) Brouwer, A. M.; Mout, R. D.; Maassen van den Brink, P. H.; van Ramesdonk, H. J.; Verhoeven, J. W.; Warman, J. M.; Jonker, S. A. *Chem. Phys. Lett.* **1991**, *180*, 556.

(7) Wasielewski, M. R. *Chem. Rev.* **1992**, *92*, 435.

(8) Brouwer, A. M.; Eijckelhoff, C.; Willemse, R. J.; Verhoeven, J. W.; Schuddeboom, W.; Warman, J. M. *J. Am. Chem. Soc.* **1993**, *115*, 2988.

(9) Van Dijk, S. I.; Wiering, P. G.; van Staveren, R.; van Ramesdonk, H. J.; Brouwer, A. M.; Verhoeven, J. W. *Chem. Phys. Lett.* **1993**, *214*, 502.

(10) Van Dijk, S. I.; Wiering, P. G.; Groen, C. P.; Brouwer, A. M.; Verhoeven, J. W.; Schuddeboom, W.; Warman, J. M. *J. Chem. Soc., Faraday Trans.* **1995**, *91*, 2107.

(11) Verhoeven, J. W.; Wegewijs, B.; Hermant, R. M.; Willemse, R. J.; Brouwer, A. M. *J. Photochem. Photobiol. A* **1996**, *95*, 3.

(12) Roest, M. R.; Verhoeven, J. W.; Schuddeboom, W.; Warman, J. M.; Lawson, J. M.; Paddon-Row, M. N. *J. Am. Chem. Soc.* **1996**, *118*, 1762.

(13) Greenfield, S. R.; Svec, W. A.; Gosztola, D.; Wasielewski, M. R. *J. Am. Chem. Soc.* **1996**, *118*, 6767.

(14) Paddon-Row, M. N. *Acc. Chem. Res.* **1994**, *27*, 18.

(15) Sauvage, J. P.; Collin, J. P.; Chambron, J. C.; Guillerez, S.; Coudret, C.; Balzani, V.; Barigelletti, F.; De Cola, L.; Flamigni, L. *Chem. Rev.* **1994**, *4*, 993.

(16) Harriman, A.; Odobel, F.; Sauvage, J. P. *J. Am. Chem. Soc.* **1995**, *117*, 9461.

(17) Treadway, J. A.; Chen, P. Y.; Rutherford, T. J.; Keene, F. R.; Meyer, T. J. *J. Phys. Chem. A* **1997**, *101*, 6824.

(18) Yonemoto, E. H.; Kim, Y. I.; Schmehl, R. H.; Wallin, J. O.; Shoulders, B. A.; Richardson, B. R.; Haw, J. F.; Mallouk, T. E. *J. Am. Chem. Soc.* **1994**, *116*, 10557.

(19) Keller, S. W.; Johnson, S. A.; Brigham, E. S.; Yonemoto, E. H.; Mallouk, T. E. *J. Am. Chem. Soc.* **1995**, *117*, 12879.

(20) Feldheim, D. L.; Grabar, K. C.; Natan, M. J.; Mallouk, T. E. *J. Am. Chem. Soc.* **1996**, *118*, 7640.

10.1021/ja983716r CCC: $19.00
Published on Web 04/04/2000

goal. At the same time it is a challenge to achieve this in an economical way, without wasting too much energy. An essential problem is therefore the estimation of the energy levels of charge-separated states in such media. The usual approach[21] is to start from the redox potentials of the electroactive groups, which are measured in a polar solvent, and to apply a correction for the smaller solvation energy in the nonpolar solvent using a crude dielectric continuum model, typically the simple Born model. Furthermore, the electrostatic interaction energy according to Coulomb's law is taken into account. The total electrostatic energy correction is typically quite large, and subject to considerable uncertainty. It is one of the purposes of the present study to obtain accurate information on the relative energies of charge-separated states, which may serve to test more detailed molecular approaches to the estimation of electrostatic solvation energies which will undoubtedly emerge soon.

In the present study we describe a few trichromophoric electron donor−donor−acceptor (D_2-D_1-A) molecules (triads) which are able to undergo stepwise charge separation in solvents of low polarity.

$$D_2-D_1-A^* \text{ (LE)} \rightarrow D_2-D_1^{+\bullet}-A^{-\bullet} \qquad \text{(CS1)}$$

$$D_2-D_1^{+\bullet}-A^{-\bullet} \text{ (CS1)} \rightarrow D_2^{+\bullet}-D_1-A^{-\bullet} \qquad \text{(CS2)}$$

The molecules are designed such that the charge separation from the locally excited (LE) state occurs very rapidly, and with nearly 100% efficiency. The second step is essentially a thermal electron transfer process, driven by the difference in oxidation potentials of the donors, but hampered by the electrostatic attraction between the charges on D_1 and A. This step has to compete with other decay processes of the CS1 state, notably charge recombination to the ground state. The first charge migration step is of crucial importance in multistep charge separation schemes, because subsequent steps tend to be easier as the change in the Coulomb energy and the rates of competing recombination processes decrease with the distance between the redox sites.

A special property of the molecules studied here is that the CS1 state is strongly fluorescent. This allows us to accurately determine the rates of the process CS1 → CS2 using stationary and time-resolved fluorescence spectroscopy. The triads studied are depicted below, together with some relevant model compounds which contain only one or two of the chromophores. In all four trichromophoric compounds (triads) a vinylcyanonaphthalene is the electron-accepting moiety (A) and a saturated amine acts as the first donor (D_1). The triads have differently substituted anilines as their second electron donor (D_2). The chromophores are linked in a linear arrangement via two saturated rings. Compound **BC3**, in which the aliphatic amino nitrogen of **TC3** is replaced by a CH group, is a bichromophoric D_2−bridge−A system designed to test the direct long-range interaction between the terminal chromophores.

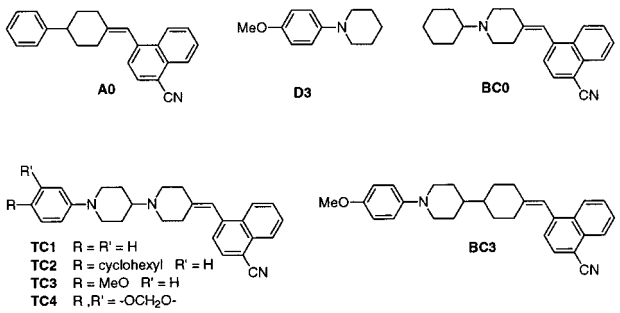

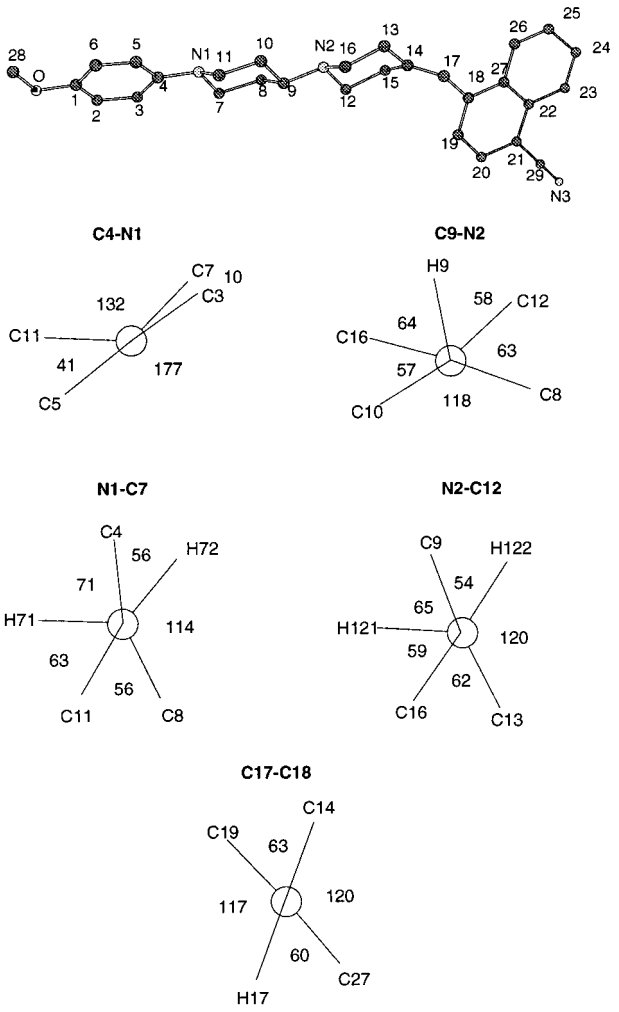

Figure 1. Structure of **TC3** as determined by single-crystal X-ray diffraction. Hydrogen atoms are omitted for clarity. Newman projections indicate dihedral angles along some relevant bonds.

It will be shown that in compounds **TC3** and **TC4** in nonpolar solvents two sequential steps of electron transfer occur upon excitation of the acceptor chromophore. Furthermore, it will be demonstrated that the rate of the second step of electron transfer is markedly dependent on solvent polarity. In general, the rate of the conversion of the CS1 state to the CS2 state tends to be faster upon increasing the dielectric constant of the medium. However, the rate of the charge migration step is relatively slower in acetates than in alkyl ethers (specific solvent effect). Moreover, we will show that the stepwise electron transfer as occurring in **TC3** is more efficient than the direct long-range electron transfer which takes place in **BC3**.

Results and Discussion

Ground State Structure. Compound **TC3** is a representative of the trichromophoric donor−donor−acceptor compound series **TC1**−**TC2**−**TC3**−**TC4**. Figure 1 shows the structure of **TC3** as determined by single-crystal X-ray diffraction as well as the Newman projections along some relevant bonds. Bond distances and bond angles of the non-hydrogen atoms of **TC3** are given in the Supporting Information.

The molecule adopts a stretched conformation with both piperidine rings in a chair conformation. Although the structure of the triads allows some rotational freedom around the long

(21) Weller, A. *Z. Phys. Chem. Neue Folge* **1982**, *133*, 93.

Table 1. Optical Absorption Data of the Triads **TC*n*** in Acetonitrile

compd	λ_{max} (nm) {ϵ_{max} (M^{-1} cm^{-1})}
TC1	236 {45 790} 314 {13 410}
TC2	236 {46 500} 315 {13 220}
TC3	236 {46 920} 314 {13 990}
TC4	236 {45 350} 314 {15 650}

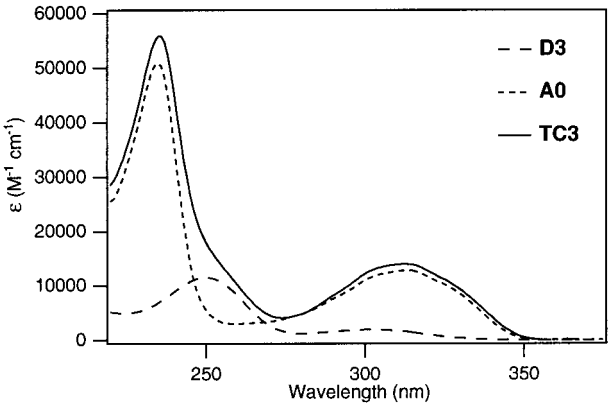

Figure 2. Representative UV absorption spectra (cyclohexane): model donor **D3**, model acceptor **A0**, and triad **TC3**.

axis of the molecules, this does not alter the distances between the chromophores. The distance between the first donor (N2) and the second donor (N1) is 4.3 Å; the edge to edge distance between the two terminal chromophores (N1−C14) is 7.2 Å. From the experimentally determined excited state dipole moments (see below), which reflect the actual charge distributions in the charge-separated states, we can calculate the corresponding distances between two unit point charges. This gives effective donor−acceptor distances $R(D_1-A) \approx 5.2$ Å and $R(D_2-A) \approx 9.7$ Å, in good agreement with the molecular structure.

Optical Absorption Spectra. The UV absorption spectra (Table 1, Figure 2) of the triads are dominated by a strong band at ca. 236 nm and a less intense absorption at ca. 314 nm. These bands can be attributed to transitions of the acceptor chromophore. In addition, a shoulder occurs at ca. 256 nm due to the aniline chromophore. The long-wavelength band of the aniline chromophores is hidden under the much stronger acceptor transition at 314 nm. Although low-energy charge transfer states must exist in the dyads and triads,[11] transitions to these states are not observed in the UV absorption spectra, probably due to a small transition probability.

Characterization of the Emissive CS1 State. Excitation of the triads at wavelengths between 308 and 320 nm leads to population of the locally excited state of the acceptor chromophore. The corresponding fluorescence (370 nm),[6] however, is completely absent, and a characteristic charge transfer (CT) emission is observed instead.[22,23] To illustrate this, the fluorescence spectra of the bichromophoric reference compound **BC0** and the **TC*n*** compounds in di-*n*-propyl ether are depicted in Figure 3. In Table 2 the maxima and the quantum yields of the CT fluorescence of the **TC*n*** systems and **BC0** in a range of solvents are listed.

The magnitude of the dipole moment of the emissive state formed upon photoexcitation can be estimated from an analysis

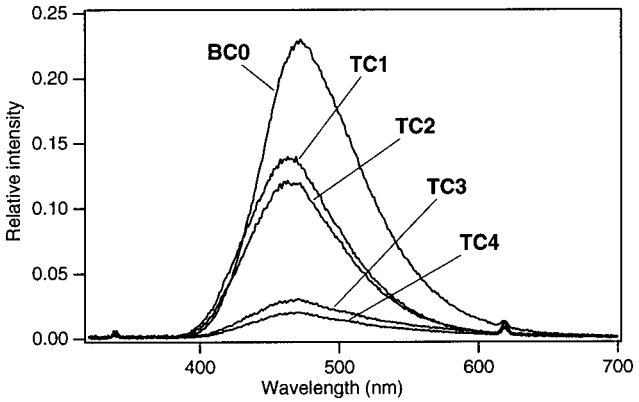

Figure 3. Fluorescence spectra of dyad **BC0** and triads **TC*n*** in di-*n*-propyl ether; excitation at 308 nm. The spectra are scaled in such a way that the maximum intensity corresponds with the fluorescence quantum yield.

of the solvatochromic shift of the emission maximum (Lippert−Mataga relation):[24−26]

$$\bar{\nu}_{CT} = \bar{\nu}^0_{CT} - \frac{2\mu^2}{\rho^3 hc}\Delta f \qquad (1)$$

In eq 1 $\bar{\nu}_{CT}$ is the wavenumber of the emission maximum of the CT band in a given solvent, $\bar{\nu}^0_{CT}$ denotes the wavenumber of the fluorescence in the gas phase, and ρ is the effective radius of a cavity which the molecule occupies in the solvent. The solvent polarity function Δf is

$$\Delta f = \frac{(\epsilon_s - 1)}{(2\epsilon_s + 1)} - \frac{(n^2 - 1)}{(4n^2 + 2)} \qquad (2)$$

Hence from the slope of a plot of $\bar{\nu}_{CT}$ vs the solvent polarity parameter Δf the magnitude of the excited state dipole moment can be estimated if the cavity radius is known.

Values for the slope and the intercept of the regression lines in the Lippert−Mataga plots shown in Figure 4 are given in Table 2. Although the emission maxima of the **TC*n*** compounds are systematically at slightly shorter wavelengths than those of the bichromophoric reference system **BC0**, all yield essentially identical values of the solvatochromic slope $2\mu^2/hc\rho^3 \approx 30\,000$ cm^{-1}. It is evident that the observed emission in all cases originates from the product of the first step of electron transfer: the $D_2D_1^+A^-$ (CS1) state. An estimate[6] of the cavity radius $\rho = 5.5$ Å leads to an estimate of the excited state dipole moment of ca. 22 D for this state. It is important to note that although dielectric continuum theory allows a useful characterization of the solvatochromic shift, a clear deviation from the ideal behavior is apparent in Figure 4. In going from diethyl ether to *n*-pentyl acetate, which have very similar Δf values, a red shift of 50 nm occurs. This specific solvent effect also affects the charge migration process, as discussed below.

Since the photophysical properties of compound **TC2** as a function of solvent and temperature have been extensively described elsewhere,[27−29] we shall now focus especially on the photophysical behavior of **TC1**, **TC3**, and **TC4**.

(22) Hermant, R. M.; Bakker, N. A. C.; Scherer, T.; Krijnen, B.; Verhoeven, J. W. *J. Am. Chem. Soc.* **1990**, *112*, 1214.
(23) Scherer, T.; Hielkema, W.; Krijnen, B.; Hermant, R. M.; Eijckelhoff, C.; Kerkhof, F.; Ng, A. K. F.; Verleg, R.; van der Tol, E. B.; Brouwer, A. M.; Verhoeven, J. W. *Recl. Trav. Chim. Pays-Bas* **1993**, *112*, 535.
(24) Lippert, E. *Z. Naturforsch. A* **1955**, *10*, 541.
(25) Mataga, N.; Kaifu, Y.; Koizumi, M. *Bull. Chem. Soc. Jpn.* **1956**, *29*, 465.
(26) Beens, H.; Knibbe, H.; Weller, A. *J. Chem. Phys.* **1967**, *47*, 1183.
(27) Willemse, R. J.; Verhoeven, J. W.; Brouwer, A. M. *J. Phys. Chem.* **1995**, *99*, 5753.
(28) Willemse, R. J. Ph.D. Thesis, University of Amsterdam, 1997.
(29) Willemse, R. J.; Verhoeven, J. W.; Brouwer, A. M. Manuscript in preparation.

Table 2. Fluorescence Maxima λ_{max} (nm) and Fluorescence Quantum Yields ϕ_f (in Square Brackets) of **BC0** and **TC*n*** Compounds in Various Solvents at Room Temperature[a]

solvent (Δf)	**BC0**	**TC1**	**TC2**	**TC3**	**TC4**
n-hexane (0.092)	419 [0.03]	412 [0.01]	411 [0.01]	412 [0.02]	410 [0.01]
cyclohexane (0.100)	420 [0.03]	413 [0.02]	413 [0.02]	413 [0.02]	411 [0.02]
di-*n*-butyl ether (0.194)	468 [0.19]	458 [0.11]	460 [0.11]	460 [0.03]	461 [0.03]
di-*n*-propyl ether (0.213)	475 [0.23]	466 [0.14]	466 [0.12]	469 [0.03]	466 [0.02]
diisopropyl ether (0.237)	481 [0.22]	472 [0.16]	472 [0.13]	470 [0.02]	468 [0.03]
diethyl ether (0.251)	496 [0.21]	483 [0.20]	486 [0.13]	485 [0.01]	484 [0.01]
n-pentyl acetate (0.259)	540 [0.06]	530 [0.10]	532 [0.06]	531 [0.01]	530 [0.01]
n-butyl acetate (0.267)	547 [0.05]	535 [0.06]	539 [0.04]	535 [0.01]	535 [<0.01]
ethyl acetate (0.292)	560 [0.01]	558 [0.02]	555 [0.01]	556 [0.01]	*b*
tetrahydrofuran (0.308)	554 [0.02]	554 [0.03]	553 [0.01]	553 [<0.01]	*b*
benzene	481 [0.31]	470 [0.19]	472 [0.21]	471 [0.07]	470 [0.05]
dioxane	517 [0.18]	504 [0.22]	503 [0.23]	506 [0.04]	507 [0.02]
intercept $\bar{\nu}_{CT}$ (0) (cm^{-1})	26900 ± 600	27500 ± 700	27500 ± 700	27400 ± 700	27300 ± 800
slope $2\mu^2/hc\rho^3$(cm^{-1})	29300 ± 2700	30500 ± 3000	30600 ± 2900	30300 ± 2900	29200 ± 3900

[a] λ_{exc} = 308 or 314 nm. The last two entries are the values of the intercept $\bar{\nu}_{CT}$ (0) (cm^{-1}) and the slope $2\mu^2/hc\rho^3$ (cm^{-1}) together with the standard deviations as obtained by linear correlation of Δf and $\bar{\nu}_{CT}$ according to eq 1. [b] No CT fluorescence observed.

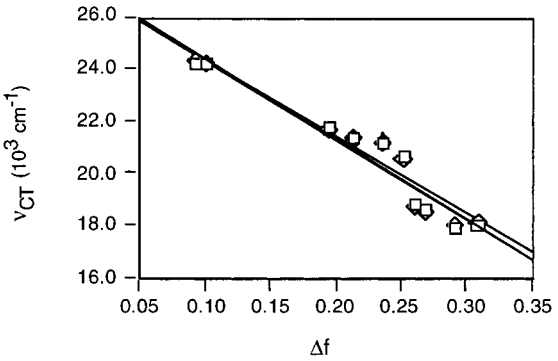

Figure 4. Lippert−Mataga plots (eq 1) for **TC1** (□) and **TC2** (◇). Data points for **TC3** and **TC4** coincide with those shown.

Radiative and Nonradiative Decay of the CS1 State in TC1, TC3, and TC4. In Table 3 the fluorescence decay times of **BC0** and the triads in a series of solvents are listed together with values of the radiative (k_f) and nonradiative (k_d) decay rates. For **TC1** the fluorescence quantum yields and decay times of the CS1 state are similar to those of the dyad **BC0**. As has been noted before for donor−acceptor systems with similar molecular structures,[22] the nonradiative decay rates are relatively high in nonpolar solvents, then decrease to reach a minimum (in this case in diethyl ether), and increase again in more polar solvents. The latter is the usual energy-gap-law behavior. The rapid decay in nonpolar solvents, in which the energy of the CS state is high, is related to the existence of an additional decay channel, as discussed elsewhere.[28,30] In the case of compounds **TC3** and **TC4** the quantum yields and decay times of the fluorescence are strongly reduced compared to the values obtained for **BC0** and **TC1**. This increased nonradiative decay of the CS1 state for **TC3** and **TC4**, which is illustrated in Figure 5, is attributed to the occurrence of the second step of electron transfer.

Not unexpectedly, we do not observe clear fluorescence from the fully charge separated (CS2) state. Due to the small electronic coupling between D_2 and A the radiative transition probability must be much smaller than for the CS1 state. For the dyad **BC3** a weak CT emission can observed, but in **TC3** the fluorescence from the CS1 state is strong enough that CS2 emission, if any, is hidden in the long-wavelength tail of the CS1 band.[28] In order to confirm the occurrence of the second step of electron transfer and to characterize the CS2 state, time-resolved microwave conductivity (TRMC)[31] and time-resolved optical absorption measurements were carried out, as described below.

On the basis of the experimentally determined free energy difference between the CS1 and CS2 states in **TC2** as a function of solvent polarity[27] we have argued that in **TC3** near-degeneracy of these states should be expected in solvents having a dielectric constant of about 2. Therefore, we carefully reinvestigated the fluorescence decays of **TC3** and **TC4** in benzene and dioxane, and indeed a weak long-lived component could be detected in these decays. This observation is attributed to feedback from the CS2 state to the CS1 state, which is slightly higher in energy.

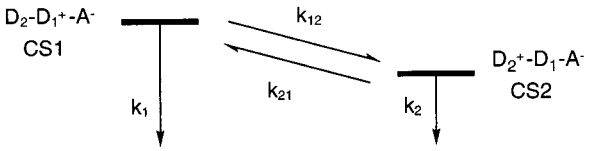

Analysis of the biexponential decay traces, using the reference compound **TC1** to estimate k_1, allows us to determine the rates of the processes depopulating the CS manifold from CS1 (k_1) and from CS2 (k_2) as well as the rates of interconversion k_{12} and k_{21}. From the equilibrium constant is obtained the free energy difference ($\Delta G_{12} = -kT \ln(k_{12}/k_{21})$). The results are given in Table 4.

Time-Resolved Microwave Conductivity (TRMC) Measurements. In order to confirm the occurrence of the second step of electron transfer in compound **TC3**, TRMC measurements were performed on compounds **BC0**, **TC1**, **BC3**, and **TC3**. The formation of the highly dipolar CS2 state should be reflected in a large change of the microwave conductivity $\Delta\sigma$ of the solution. The TRMC measurements were carried out and analyzed as fully described elsewhere.[31,32] The amplitude of the observed TRMC signal was analyzed to yield the conductivity parameter $\mu_{CS}^2\phi_{CS}/\theta$, in which μ_{CS} represents the excited state dipole moment, ϕ_{CS} is the quantum yield of formation of the dipolar species, and θ is the rotational relaxation time. From the conductivity parameter we can calculate the excited state dipole moment if ϕ_{CS} and θ are known.

Figure 6 shows the TRMC traces for **BC0**, **TC1**, **TC3**, and **BC3** in benzene and dioxane. The signal intensities in dioxane

(30) Willemse, R. J.; Theodory, D.; Mout, R. D.; Verhoeven, J. W.; Brouwer, A. M. Manuscript in preparation.

(31) de Haas, M. P.; Warman, J. M. *Chem. Phys.* **1982**, *73*, 35.

(32) Schuddeboom, W. Ph.D. Thesis, Delft University of Technology, 1994.

Table 3. Fluorescence Lifetimes (τ_f) (ns) and Radiative (k_f) and Nonradiative (k_d) Decay Rates (10^7 s^{-1}) of Dyad **BC0** and Triads **TC*n*** in Various Solvents at Room Temperature[a]

	BC0				TC1				TC3				TC4			
solvent (ϵ_s)	ϕ_f	τ_f	k_f	k_d	ϕ_f	τ_f	k_f	k_d	ϕ_f	τ_f	k_f	k_d	ϕ_f	τ_f	k_f	k_d
benzene (2.28)	0.31	6.16	5.0	11	0.19	2.84	6.7	29	0.07	0.91[d]	7.7	102	0.05	0.79[d]	6.3	120
dioxane (2.21)	0.18	6.71	2.7	12	0.22	6.17	3.6	13	0.04	1.56[d]	2.6	62	0.02	1.26[d]	1.6	78
di-*n*-butyl ether (3.06)	0.19	4.02	4.7	20	0.11	1.92	5.7	46	0.03	0.58	5.2	167	0.03	*b*		
di-*n*-propyl ether (3.39)	0.23	4.20	5.5	18	0.14	3.13	4.5	27	0.03	0.46	6.5	211	0.02	0.40	5.0	245
diisopropyl ether (3.88)	0.22	6.38	3.4	12	0.16	3.79	4.2	22	0.02	0.38	5.3	258	0.02	0.33	6.1	297
diethyl ether (4.24)	0.21	7.40	2.8	11	0.20	5.10	3.9	16	0.01	0.39	2.6	254	0.01	0.35	2.9	283
n-pentyl acetate (4.75)	0.06	2.98	2.0	32	0.10	3.56	2.8	25	0.01	0.92	1.1	108	0.01	0.96	1.0	103
n-butyl acetate (5.01)	0.05	2.16	2.3	44	0.06	2.94	2.0	32	0.01	0.76	1.3	130	<0.01	0.75	1.3	132
ethyl acetate (6.00)	0.01	1.21	0.8	82	0.02	1.72	1.2	57	0.01	0.55	1.8	180	*c*			

[a] Excitation at wavelengths between 315 and 320 nm. [b] Not measured. [c] No CT fluorescence observed. [d] Biexponential fluorescence decays are observed in benzene and dioxane for **TC3** and **TC4**; only the fastest component which has by far the highest amplitude is given.

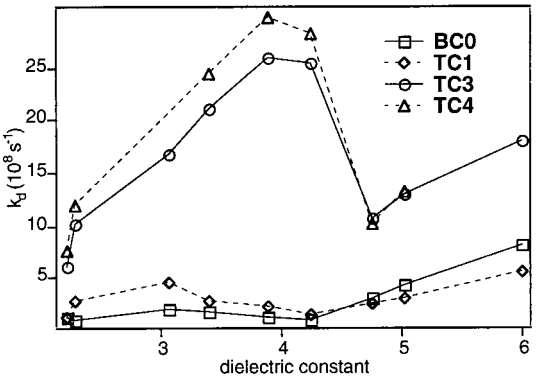

Figure 5. Nonradiative decay rates of **BC0** and **TC*n*** compounds in a series of solvents arranged according to their dielectric constant.

Table 4. Rate Constants (10^8 s^{-1}) Characterizing the Decay Processes in **TC3** and **TC4** in Benzene and Dioxane from Time-Resolved Fluorescence Measurements

compd	solvent (ϵ_s)	λ_{det} (nm)	k_1	k_2	k_{12}	k_{21}	K_{eq}	ΔG_{12} (eV)
TC3	benzene (2.28)	470	3.5	0.7	7.0	0.5	13	−0.07
TC3	dioxane (2.21)	500	1.6	0.4	4.7	0.1	40	−0.09
TC4	benzene (2.28)	470	3.5	0.8	8.8	0.4	23	−0.08
TC4	dioxane (2.21)	500	1.6	0.8	6.2	0.2	34	−0.09

were scaled to correct for the difference in viscosity between benzene and dioxane, which influences the rotational relaxation time θ. For all four compounds large dipolar transient signals were observed upon flash photolysis. The data could be fitted with a single dipolar intermediate and a small underlying slowly decaying signal close to the noise level. For **TC3** a small additional short-lifetime component was included in the final fitting procedure to take into account the presence of the CS1 state. The values of the lifetimes of the dipolar intermediates and the corresponding values of the conductivity parameter $\mu_{CS}^2\phi_{CS}/\theta$ are compiled in Table 5. For **BC0** and **TC1** the dipole moments in Table 5 were calculated using estimates of the dipolar relaxation times and based on a quantum yield of unity for the formation of the CS1 state. For **TC3** quantum yields of formation of the CS2 state of 0.68 and 0.75 in benzene and dioxane, respectively, as derived from the quenching of the CS1 fluorescence, were used to calculate the dipole moments in Table 5.

From the TRMC transient observed for **BC0** was determined a dipole moment of 23 D. This value is in good agreement with the value of ca. 22 D derived from the solvatochromic shift. The TRMC measurements on **TC1** yielded a dipole moment on photoexcitation of approximately 26 D, which is similar to

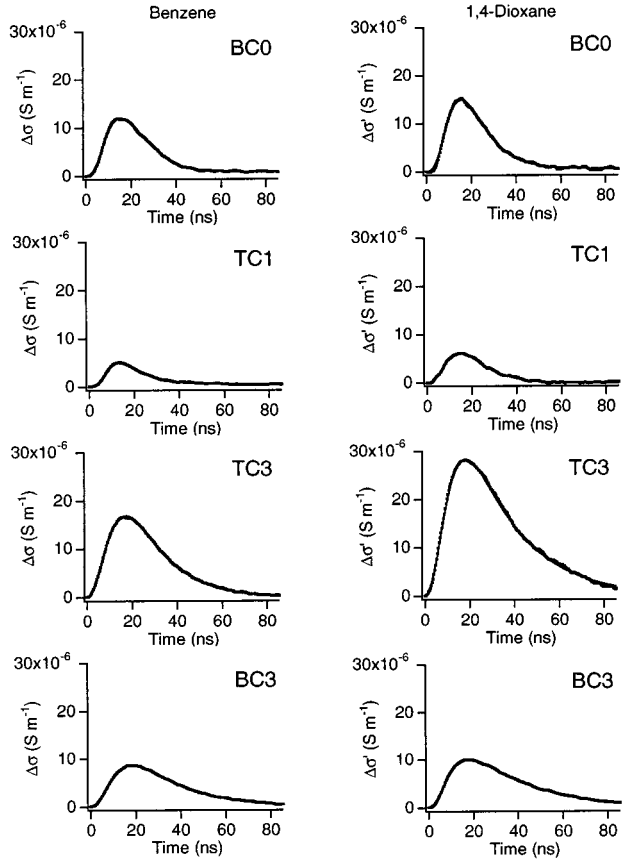

Figure 6. Time-resolved microwave conductivity transients $\Delta\sigma$ observed on flash photolysis of benzene and 1,4-dioxane solutions of the compounds **BC0**, **TC1**, **TC3**, and **BC3**. The full lines are convolution fits to the experimental data (dotted lines). The transients in dioxane are scaled 2.25× to correct for the difference in viscosity between benzene and dioxane.

the value found for **BC0**. If the second step of electron transfer had occurred, a significantly larger value would have been expected. The fact that the magnitude of the TRMC transient for **TC1** is in fact considerably smaller than that for **BC0** as shown in Figure 6 is a result of the much longer rotation time for the former molecule.

In the case of compound **TC3** the observed signal is seen to be much larger than for **TC1** even though the rotation time for the former should be even longer. Even based on a maximum quantum yield of unity the dipole moment of the species responsible for the TRMC signal of **TC3** would be estimated to be ca. 40 D, i.e., much larger than for **BC0** or **TC1**. It can therefore be concluded that for **TC3** the second electron transfer

Table 5. Lifetime τ_{CS}, Conductivity Parameter $\mu_{CS}^2\phi_{CS}/\theta$, Rotational Relaxation Time θ, Quantum Yield ϕ_{CS}, and the Calculated Dipole Moment μ_{CS} as Obtained from the TRMC Measurements Using Benzene (BZ) and Dioxane (DX) as Solvents

	τ_{CS} (ns)		$\mu_{CS}^2\phi_{CS}/\theta$ (D^2/ps)		θ^a (ps)		ϕ_{CS}		μ_{CS} (D)	
compd	BZ	DX	BZ	DX	BZ	DX	BZ	DX	BZ	DX
BC0	7	7	1.91	0.85	277	619	1	1	23	23
TC1	3	6.5	1.59	0.66	458	1022	1	1	27	26
TC3	14	23	2.44	1.49	545	1216	0.68[b]	0.75[b]	44	49
BC3	19	26	1.14	0.55	542	1209	0.32[c]	0.28[c]	44	49

[a] Reference 32. [b] Derived from fluorescence results according to $\phi_{12} = 1 - (\tau_{TC3}/\tau_{TC1})$. [c] Based on the assumption that the dipole moments of the fully charge separated states of **BC3** and **TC3** are equal.

step undoubtedly occurs, leading to the highly dipolar CS2 state. When the values for the quantum yields of the formation of the CS2 state in benzene and dioxane are used in the analysis of the TRMC transients, dipole moments of the CS2 state of 44 and 49 D are found, respectively. The increase in dipole moment compared with compounds **BC0** and **TC1** corresponds to an extra charge separation distance of ca. 4 Å, which is close to the distance between the nitrogen atoms of the two donor groups as determined in the X-ray crystal structure of **TC3**. From the TRMC signals the lifetimes of the CS2 state in benzene and dioxane are found to be 14 and 23 ns, respectively, considerably longer than those of the fluorescent intermediate CS1 state.

In the case of compound **BC3** the observation of a large dipolar transient indicates the formation of the long-range charge-separated state (D_2^+−bridge−A^-), although the observed signal is seen to be much smaller for **BC3** than for **TC3**. Assuming now that the conformations and the dipole moments of the fully charge separated states of **TC3** and **BC3** are the same, the quantum yields for charge separation in **BC3** can be estimated from the results on **TC3**. The values obtained for ϕ_{CS} in **BC3** are listed in Table 5.

Characterization of the CS2 State by Time-Resolved Optical Absorption Measurements. Spectra of the Radical Ions of the Separate Chromophores. It is reasonable to expect the optical absorption spectra of the ion-pair-like CS states to resemble a superposition of the spectra of the constituent radical ions. The model acceptor compound **A0** is reversibly reduced in acetonitrile at $E_{1/2} = -1.75$ V vs SCE ($T = 293$ K, $\upsilon \geq 100$ mV/s). Therefore, the UV−vis absorption spectrum of the radical anion could be conveniently recorded after electrochemical reduction of **A0** in an OTTLE cell[33] (see Figure 7). The radical anion of **A0** displays two absorption bands in the visible spectrum: a strong absorption band at 446 nm ($\epsilon = 15\,500$ M^{-1} cm^{-1}) with a shoulder at 507 nm ($\epsilon = 4800$ M^{-1} cm^{-1}) and a weak absorption at 735 nm ($\epsilon = 2500$ M^{-1} cm^{-1}). The latter absorption is in a wavelength region where no spectral overlap exists between the absorptions of $\mathbf{A}^{-\bullet}$, $\mathbf{D}^{+\bullet}$, and $^3\mathbf{A}^*$ in the donor−acceptor systems studied. Hence, monitoring the transient absorption in this wavelength region can in principle give accurate information about the kinetics of the charge-separated state, even though the radical anion does not absorb very strongly.

Oxidation of the model donor compound **D3**, studied by means of cyclic voltammetry in acetonitrile, is a chemically reversible one-electron process at $E_{1/2} = 0.61$ V vs SCE at room temperature and $\upsilon \geq 100$ mV/s. The methylenedioxy derivative **D5** is a slightly better electron donor, with $E_{1/2} = 0.57$ V under the same conditions. The radical cations of **D3** and **D5**, unfortunately, were found to be unstable at room temperature on the time scale of the spectroelectrochemical measurements (10−100 s). Their spectra could, however, be readily observed when the radical cations were generated as transient species by using a cosensitization technique[34,35] with nanosecond time-resolved detection. The spectrum obtained for $\mathbf{D3}^{+\bullet}$ (a broad band with maxima at 480 and 505 nm, see Figure 7) is in agreement with the spectra reported for the radical cations of *N*-(4-methoxyphenylpiperidine) (λ_{max} 505 nm ($\epsilon = 6000$ M^{-1} cm^{-1}))[6] and *N*,*N*-dimethyl-4-methoxyaniline (λ_{max} 470 and 490 nm).[36] This absorption feature was also found in the UV−vis spectrum of $\mathbf{D3}^{+\bullet}$ electrogenerated in butyronitrile at −80 °C, but additional bands were also present in this spectrum, possibly due to secondary products.

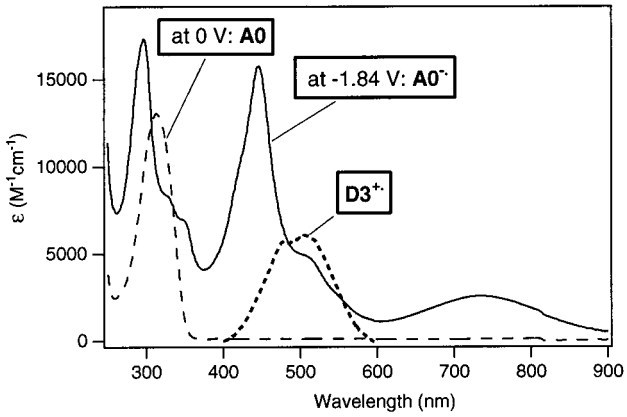

Figure 7. UV−vis absorption spectra of **A0** (dashed lines) and its radical anion (full line, produced by electrochemical reduction at room temperature) in butyronitrile. The spectrum of the radical cation of **D3** (dotted line; cosensitization experiment, CH_3CN) is included, scaled to $\epsilon_{max} = 6000$ M^{-1} cm^{-1}.[6]

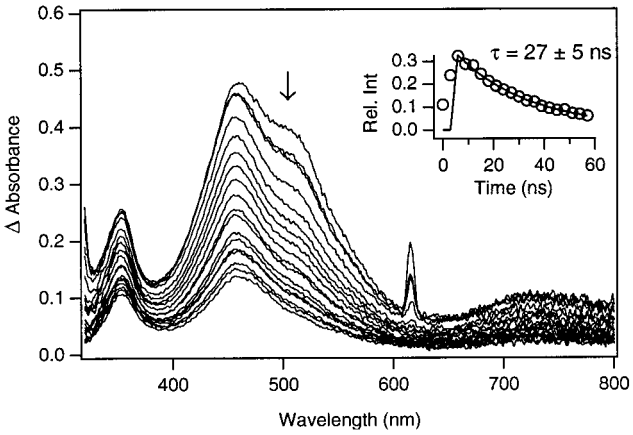

Figure 8. Transient absorption spectra of **TC3** in dioxane. The first spectrum shown was taken at the maximum of the exciting laser pulse, the subsequent ones with time increments of 3 ns. Inset: decay of transient absorption integrated between 490 and 560 nm.

Nanosecond Time-Resolved Optical Absorption Measurements. Having determined the radical ion reference spectra, we could further characterize the CS2 state in **TC3** by time-resolved optical absorption measurements. Figure 8 shows the transient absorption spectra of **TC3** in dioxane as an example. Very similar spectra were obtained in benzene or diethyl ether. At short times after the exciting pulse a strong band at ca. 460 nm

(33) Krejcik, M.; Danek, M.; Hartl, F. *J. Electroanal. Chem. Interfacial Electrochem.* **1991**, *317*, 179.

(34) Majima, T.; Pac, C.; Nakasone, A.; Sakurai, H. *J. Am. Chem. Soc.* **1981**, *103*, 4499.

(35) Mattes, S. L.; Farid, S. *Acc. Chem. Res.* **1982**, *15*, 80.

(36) Hester, R. E.; Williams, K. P. J. *J. Chem. Soc., Perkin Trans. 2* **1982**, 559.

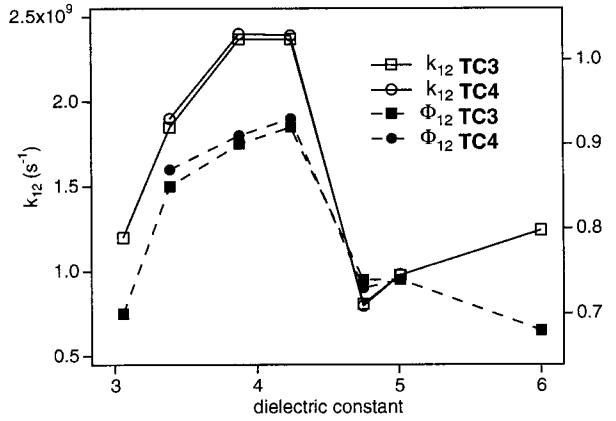

Figure 9. Rates of the second electron transfer step, k_{12}, as calculated from eq 3 (left axis) and quantum yield of formation of the CS2 state as calculated from eq 4 (right axis) as a function of the dielectric constant.

and a weak band at ca. 730 nm are observed. The former corresponds to a superposition of bands of the 1-(4-methoxyphenyl)piperidine radical cation (**D3**$^{+\bullet}$) and the acceptor radical anion (**A0**$^{-\bullet}$); the long-wavelength band is characteristic of the acceptor radical anion. Unfortunately, the time resolution of our equipment is insufficient to observe the conversion of CS1 to CS2 (time scale < 2 ns). This should lead to a clear increase of the absorption around 500 nm, because saturated amine radical cations such as **D1**$^{+\bullet}$ do not absorb strongly in the visible.[37]

At longer times the CS species have decayed, and two bands (355, 470 nm) of the local triplet state of the acceptor chromophore[28,30] remain. Thus, the charge-separated states decay to a local triplet state as well as to the ground state. The latter pathway is dominant (>85%). The bands attributed to the CS2 state decay with time constants similar to those of the TRMC signals. A corresponding band of an aniline radical cation fragment is not observed in the case of **TC1** (spectra not shown). The highly fluorescent CS1 state (with a lifetime of ca. 6 ns) decays to a local triplet of the acceptor as well as to the ground state. These results provide further confirmation that the second electron transfer step does occur in **TC3**, but not in **TC1**.

Efficiency of the Second Electron Transfer Step. From the increased nonradiative decay rate of the CS1 state in **TC3** and **TC4** compared to **TC1**, the rate of the second electron transfer step, k_{12}, and the quantum yield of formation of the CS2 state, ϕ_{CS2}, can be calculated using eqs 3 and 4 under the assumption of irreversibility of the second step of electron transfer:

$$k_{12} = \frac{1}{\tau_{\mathbf{TC}n}} - \frac{1}{\tau_{\mathbf{TC1}}} \quad (3)$$

$$\phi_{CS2} = 1 - \frac{\tau_{\mathbf{TC}n}}{\tau_{\mathbf{TC1}}} \quad (4)$$

Figure 9 depicts the rate of the second electron transfer step and the quantum yield of the CS2 state as a function of the dielectric constant.

As can be seen, the stepwise charge separation in compounds **TC3** and **TC4** is realized with an efficiency of about 70% in di-*n*-butyl ether, increasing to more than 90% in more polar alkyl ethers. This increased efficiency is caused by the fact that the second electron transfer step becomes faster as a result of the increased stabilization of the CS2 state relative to the CS1 state at higher solvent polarity. Moreover, the charge recombination in the CS1 state becomes slower upon increasing the dielectric constant (see Table 3), which further contributes to the increased efficiency of the second charge transfer step.

Remarkably, in the acetates the formation of the CS2 state is less efficient. The reason is 2-fold: the nonradiative charge recombination in the CS1 state is faster in acetates than in alkyl ethers (see Table 3), while the rate of the second step of electron transfer is slower in acetates compared to alkyl ethers (see Figure 9). As noted above, the changes in the position of the emission maxima also indicated that the solvation of the CS1 state in **BC0** and the **TC*n*** compounds is relatively better in acetates than in ethers. The fact that the rate of the conversion of the CS1 state into the CS2 state is relatively slower in acetates indicates that this especially favored solvation applies only to the CS1 state and not (or to a lesser extent) to the CS2 state.

The bulk dielectric properties are clearly not sufficient to fully describe the solvent effects observed. Details of the microscopic solvation must be studied to understand this phenomenon. Preliminary Monte Carlo simulations indicate that it is possible for the alkyl acetate solvents, which have their dipolar group on one end of the molecule, to line up with the CS1 dipole in such a way that both ends of the solvent dipole interact simultaneously with D^+ and A^-. The symmetric alkyl ethers, which have their polar group embedded in the middle of the molecule, cannot do this. For the CS2 state, the distance between D_2^+ and A^- is so large that a single acetate molecule cannot interact effectively with both sites, and as a result the solvation is like that of a pair of ions.

Long-Range Electron Transfer vs Stepwise Electron Transfer. The trichromophoric compounds were designed in order to accomplish a charge separation over a large distance via a stepwise electron transfer mechanism. In principle, direct long-range electron transfer between the terminal chromophores could occur. In compound **BC3**, in which the aliphatic amino nitrogen is replaced by a CH group, the electron transfer must occur as a single-step process. According to the TRMC results, the yield of the charge-separated state is ca. 30% in benzene and dioxane (Table 5). In compound **TC3**, on the other hand, two steps of electron transfer occur sequentially upon excitation, leading to a yield of ca. 70% of the CS2 state in the same solvents. The reduced quantum yield of emission of the CS1 state of **TC3** and **TC4** relative to **TC1** could have been caused by direct long-range electron transfer $D_2-D_1-A^* \rightarrow D_2^+-D_1-A^-$, but the fact that the lifetime is decreased proportionally shows that there is indeed an additional decay path of CS1, which is ca. 100% populated as it is in **BC0**. From the fact that for compound **BC3** residual local fluorescence is observed, we conclude that the direct long-range electron transfer between the terminal chromophores takes place on the same time scale as the local decay processes of the initially excited chromophore (ca. 6×10^{10} s^{-1}).[28,30] For **TC3**, on the other hand, no residual local fluorescence is observed, indicating that the first step of electron transfer (LE → CS1) is much faster than direct long-range electron transfer between the terminal chromophores (LE → CS2). From these results it can be concluded that in nonpolar solvents the stepwise electron transfer as occurring in **TC3** is ca. three times more efficient than the long-range electron transfer which takes place in **BC3**.

Driving Force of Charge Migration. The estimation of the energies of polar excited states in solvents of low polarity is a long-standing problem in the field. The systems studied in this work have allowed us to obtain quantitative information on the interconversion rates and the relative energies of two different

(37) Shida, T. *Electronic absorption spectra of radical ions*; Elsevier: Amsterdam, 1988.

CS states in the same molecule, which was an important goal of the present study.[27] A charge-separated species with a sufficiently large donor−acceptor distance, such as the CS2 state in our triads, is quite well described by the commonly used model of an intramolecular radical ion pair. The observation that the transient absorption spectrum of **TC3** closely resembles the superposition of the spectra of the D_2^+ and A^- model systems supports the idea that the radical ion pair picture is realistic even in solvents of quite low polarity such as benzene or dioxane. For such an ion pair, in which D^+ and A^- are considered to be individually and independently solvated, the energy ΔG_{CS2} (relative to the neutral ground state) may be estimated using the redox potentials, measured in a polar solvent with dielectric constant ϵ_{polar}, the Coulomb interaction energy between unit charges at the distance D_2−A, and a correction for the ion solvation energy based on the Born model:

$$\Delta G_{CS2} = E^{ox}_{D_2} - E^{red}_{A} - \frac{14.4}{\epsilon_s R_{D_2A}} + 14.4\left(\frac{1}{2r^{ion}_{D_2}} + \frac{1}{2r^{ion}_{A}}\right)\left(\frac{1}{\epsilon_s} - \frac{1}{\epsilon_{polar}}\right) \quad \text{(eV)} \quad (5)$$

The application of this model to CS1 and CS2, neglecting possible differences in the Born ion radii of the donors, leads to a simple expression for the free energy change of the charge migration step as a function of the dielectric constant ϵ_s:

$$\Delta G_{12} = \Delta G_{CS2} - \Delta G_{CS1} = E^{ox}_{D_2} - E^{ox}_{D_1} - \frac{14.4}{\epsilon_s}\left(\frac{1}{R_{D_2A}} - \frac{1}{R_{D_1A}}\right) \quad \text{(eV)} \quad (6a)$$

On the basis of the experimentally determined dipole moments and the molecular structure we can estimate the distances as $R_{D_2A} \approx 9.7$ Å and $R_{D_1A} \approx 5.2$ Å. This leads to a predicted slope of a plot of ΔG_{12} versus $1/\epsilon_s$ of ca. 1.3 eV (eq 6b):

$$\Delta G_{12} = E^{ox}_{D_2} - E^{ox}_{D_1} + \frac{1.3}{\epsilon_s} \quad \text{(eV)} \quad (6b)$$

As we have previously shown,[27] the experimental data for **TC2** in a series of ethers give

$$\Delta G_{12} = E^{ox}_{D_2} - E^{ox}_{D_1} + \frac{0.6}{\epsilon_s} \quad \text{(eV)} \quad (6c)$$

Equation 6b predicts $\Delta G_{12} \approx +0.25$ eV for **TC3** ($E^{ox}_{D_2} - E^{ox}_{D_1} \approx -0.32$ V)[27] in benzene and dioxane, which is clearly incorrect, as we now experimentally find $\Delta G_{12} = -0.07$ and -0.09 eV, respectively, in these solvents. This result, on the other hand, is completely consistent with the empirical relation (6c) found for **TC2**, which also correctly predicts that in dibutyl ether and more polar solvents ΔG_{12} is sufficiently negative (< -0.12 eV) that the charge shift process is irreversible.

Thus, our experimental results show that formation of the very polar CS2 state from the less polar CS1 state in a nonpolar solvent is much more facile than expected from the simple model which led to eq 6b. The major reason for the discrepancy is probably that the ion-pair description of the CS1 state is invalid because the solvation spheres of the donor and acceptor ions overlap considerably. Thus, counting both the ion solvation terms and the Coulombic interaction energy to their full extent leads to an underestimation of the energy of the CS1 state.

A nonnegligible difference in the Born ion radii of D_1 and D_2 could also contribute to the discrepancy. If we, for example, assume that $r_{D_2} = 4.5$ Å and $r_{D_1} = 3.5$ Å, the value for the expected slope is 0.72 eV. The aniline donor may indeed be somewhat larger in size than the saturated amine. We tested this hypothesis by means of quantum-chemical calculations of the continuum solvation energy of radical cations of cyclohexylpiperidine (D_1 model) and *N*-phenylpiperidine (D_2 model). Using the self-consistent isodensity polarized continuum method[38,39] with a dielectric constant of 78.5 we found solvation energies of 48.7 and 48.3 kcal/mol, respectively, at the HF/6-31G(d) level, and 47.4 and 47.1 kcal/mol, respectively, using density functional theory (BLYP/6-31G(d)).[40] The corresponding Born ion radius would be ca. 3.7 Å for both radical cations. Although there may still be considerable uncertainty as to the reliability of the computational model used, the result clearly indicates that the *difference* in solvation energies of D_1 and D_2 radical cations is likely to be small.

Another factor to consider is that the assumption of full charge separation for the CS1 state may not be correct. It is well-known that mixing occurs of the CS1 charge-separated configuration with a locally excited state of the acceptor chromophore.[41] Although this may reduce the dipole moment and thus the electrostatic price to be paid in the transition CS1 → CS2, it should lead to electronic stabilization of CS1 especially in nonpolar media, which makes the conversion to CS2 more difficult.

The simple ion-pair model may be appropriate for the CS2 state, but for the CS1 state a description in terms of a dipole solvation model is probably more suitable. In fact this is what we did above when we analyzed the solvatochromic shift data using the Lippert−Mataga method, which is based on the Kirkwood−Onsager[42] model of solvation. The energy of the CS1 state (ΔG_{CS1}) can be estimated as shown in eq 7. The factor

$$\Delta G_{CS1} = \Delta G^0_{CS1} - \frac{\mu^2}{\rho^3}\frac{(\epsilon_s - 1)}{(2\epsilon_s + 1)} \quad (7)$$

μ^2/ρ^3 is known from the analysis of the solvatochromic shift of the emission maxima of the triads to be ca. 15 000 cm^{-1} (1.86 eV) (see Table 2). We assume that the energy of the CS2 state (ΔG_{CS2}) can be appropriately described by the Born approach, eq 5. Combination of eqs 5 and 7 (using an average Born ion radius for D_2 and A) gives an expression for the difference in energy (ΔG_{12}) between both charge-separated states as a function of ϵ_s:

$$\Delta G_{12} = \text{constant} + \frac{14.4}{\epsilon_s}\left(\frac{1}{r^{av}_{ion}} - \frac{1}{R_{D_2A}}\right) + \frac{\mu^2}{\rho^3}\frac{(\epsilon_s - 1)}{(2\epsilon_s + 1)} \quad (8)$$

Two different functions of the dielectric constant ϵ_s appear in eq 8, but they are almost linearly related: over the polarity range of interest ($\epsilon = 2-10$) the linear relationship $(\epsilon_s - 1)/(2\epsilon_s + 1) = 0.478 - 0.5678(1/\epsilon_s)$ holds within 3%. Thus, we arrive at eq

(38) Foresman, J. B.; Keith, T. A.; Wiberg, K. B.; Snoonia, J.; Frisch, M. J. *J. Phys. Chem.* **1996**, *100*, 16098.
(39) Miertus, S.; Scrocco, E.; Tomasi, J. *Chem. Phys.* **1981**, *55*, 117.
(40) Frisch, M. J.; Trucks, G. W.; Schlegel, H. B.; Gill, P. M. W.; Johnson, B. G.; Robb, M. A.; Cheeseman, J. R.; Keith, T.; Petersson, G. A.; Montgomery, J. A.; Raghavachari, K.; Al-Laham, M. A.; Zakrzewski, V. G.; Ortiz, J. V.; Foresman, J. B.; Cioslowski, J.; Stefanov, B. B.; Nanayakkara, A.; Challacombe, M.; Peng, C. Y.; Ayala, P. Y.; Chen, W.; Wong, M. W.; Andres, J. L.; Replogle, E. S.; Gomperts, R.; Martin, R. L.; Fox, D. J.; Binkley, J. S.; Defrees, D. J.; Baker, J.; Stewart, J. J. P.; Head-Gordon, M.; Gonzalez, C.; Pople, J. A. *Gaussian 94*; Gaussian, Inc.: Pittsburgh, PA, 1995.
(41) Bixon, M.; Jortner, J.; Verhoeven, J. W. *J. Am. Chem. Soc.* **1994**, *116*, 7349.
(42) Onsager, L. *J. Am. Chem. Soc.* **1936**, *58*, 1486.

9. Using the numerical values of $R_{D_2A} = 9.7$ Å and $\mu^2/\rho^3 =$

$$\Delta G_{12} = \text{constant} + \left\{14.4\left(\frac{1}{r_{\text{ion}}^{\text{av}}} - \frac{1}{R_{D_2A}}\right) - 0.57\left(\frac{\mu^2}{\rho^3}\right)\right\}\frac{1}{\epsilon_s} \quad (9)$$

1.86 eV and the experimental dependence of ΔG_{12} on $1/\epsilon$ (eq 6c), we find that an average ion radius of D_2 and A of 4.6 Å fits the data. This seems a rather large value, compared to the range of values found in the literature for related organic donors and acceptors[10,13,21,43] and the value estimated from the quantum-chemical calculation above. Thus, while eq 8 can successfully account for the experimental observations, it is based on a rather arbitrary mix of models and requires an assumption of an ionic radius that is rather large. Obviously, there is a need for a consistent model that describes both states on an equal footing.

The current use of solvation models in the electron transfer field is in general very simplistic. We believe that in principle modern computational chemistry can offer much improvement,[44] but we note the following key problems.

(1) Solute electronic structure and electrostatic potential: We (and others) have used a dipole or two point charges in idealized cavities. The use of a multisite model representing the charge distribution, a realistic cavity shape, or separate cavities for the slow and fast solvent responses[45,46] will be an improvement. Unfortunately, it is currently not straightforward to derive the charge distribution of charge-separated excited states, including the effect that the medium will have on the charge distribution. In principle, the quantum chemical framework is available for computing the excited state structures and wave functions.[47,48] The inclusion of medium effects via dielectric continuum theory is also possible.[49] Practical implementations at ab initio levels, however, are limited to relatively small systems, while the accuracy of lower-level semiempirical quantum chemical methods remains to be established.

(2) Solvent properties: It is clear from the present study that the dielectric continuum description of a solvent can be grossly inadequate. On the other hand, it has the advantage that it is easy to apply. The use of simulations based on microscopic models of solvents has become almost routinely accessible to many chemists and could in principle become a standard tool in the electron transfer field.[50] For accurate results with solvents of low polarity, solvent polarizability must be included. At this moment, there are no established and widely available procedures for doing this.

Accurate description of the solute and the solvent being already difficult, a truly detailed model treating both at the same level is not likely to be within reach. On the other hand, it is desirable that a practical "semiempirical" approach is developed which does not require heavy computation. Accurate experimental data are required for this purpose, and we hope that our present work has made a useful contribution to this.

Concluding Remarks

We have shown that in the triad systems **TC3** and **TC4** two steps of electron transfer can occur upon excitation of the acceptor chromophore. The first charge-separated $D_2-D_1^+-A^-$ (CS1) state can be detected by means of time-resolved fluorescence spectroscopy, and the fully charge separated $D_2^+-D_1-A^-$ (CS2) state, which is formed from CS1 via a charge shift, by time-resolved microwave conductivity and transient optical absorption measurements. Furthermore, we have demonstrated that the rate of the charge shift is markedly dependent on solvent polarity. In general, the rate of the conversion of the CS1 state to the CS2 state tends to be faster upon increasing the dielectric constant of the medium. However, the rate of the charge migration step is relatively slower in acetates than in alkyl ethers (specific solvent effect). Moreover, we showed that the stepwise electron transfer as occurring in **TC3** is more efficient than the direct long-range electron transfer which takes place in **BC3**.

The electrostatic continuum models commonly used for estimating the energies of CS states fail to predict correctly the relative energies of CS1 and CS2 in low-polarity solvents: contrary to the simple model prediction ($\Delta G_{12} \approx +0.25$ eV), the driving forces found in benzene ($\Delta G_{12} \approx -0.07$ eV) and dioxane ($\Delta G_{12} \approx -0.09$ eV) are sufficient for the charge migration to proceed.

Experimental Section

Descriptions of the synthetic methods used and details of the syntheses and characterizations are available in the Supporting Information.

Optical Absorption Spectroscopy. Electronic absorption spectra were recorded on a Hewlett-Packard 8451 A or 8453 diode array spectrophotometer or on a Cary 3 (Varian). Molar absorption coefficients were determined using concentrations of $10^{-4}-10^{-5}$ M. Commercially available spectrograde solvents were used.

Steady State Fluorescence Measurements. Fluorescence spectra were recorded on a Spex Fluorolog II emission spectrometer using an RCA-C31034 GaAs photomultiplier as detector. Fluorescence spectra were corrected for the wavelength dependent response of the detection system. Fluorescence quantum yields were determined relative to a reference solution (9,10-diphenylanthracene in cyclohexane ($\phi = 0.90$),[51] quinine bisulfate in 1 N sulfuric acid ($\phi = 0.546$),[51] or triphenylene in cyclohexane ($\phi = 0.08$)[52]) and corrected for the refractive index of the solvent. The samples were made with an absorbance between 0.1 and 0.2 (1 cm path length) at the excitation wavelength and were deoxygenated by purging with argon for 10−15 min. Commercially available spectrograde solvents were used (Merck, Uvasol), except for di-*n*-butyl ether (Merck, better than 99%, washed three times with H_2SO_4). When the purity of the solvent was found to be insufficient, the solvent was purified by standard procedures.[53] All alkyl ethers were distilled from CaH_2 or $LiAlH_4$ prior to use. All acetates were washed with a saturated Na_2CO_3 solution and distilled from CaH_2.

Time-Resolved Fluorescence Measurements. Fluorescence decay curves were measured by means of picosecond time-correlated single photon counting (SPC). The experimental setup has been fully described elsewhere.[10] A mode-locked argon ion laser (Coherent 486 AS Mode Locker and Coherent Innova 200 laser) was used to pump synchronously a DCM dye laser (Coherent model 700). The output frequency was doubled with a BBO crystal resulting in 310−320 nm pulses. A Hamamatsu microchannel plate photomultiplier (R3809) was used as detector. The response function (fwhm ca. 20 ps) was obtained by

(43) van Dijk, S. I.; Groen, C. P.; Hartl, F.; Brouwer, A. M.; Verhoeven, J. W. *J. Am. Chem. Soc.* **1996**, *118*, 8425.
(44) Cramer, C. J.; Truhlar, D. G. *Chem. Rev.* **1999**, *99*, 2161.
(45) Basilevsky, M. V.; Rostov, I. V.; Newton, M. D. *Chem. Phys.* **1998**, *232*, 189.
(46) Newton, M. D.; Basilevsky, M. V.; Rostov, I. V. *Chem. Phys.* **1998**, *232*, 201.
(47) Merchán, M.; Serrano-Andrés, L.; Gonzalez-Luque, R.; Roos, B. O.; Rubio, M. *Theochem—J. Mol. Struct.* **1999**, *463*, 201.
(48) Christiansen, O.; Gauss, J.; Stanton, J. F.; Jørgensen, P. *J. Chem. Phys.* **1999**, *111*, 525.
(49) Barone, V.; Cossi, M.; Tomasi, J. *J. Comput. Chem.* **1998**, *19*, 404.
(50) Ungar, L. W.; Newton, M. D.; Voth, G. A. *J. Phys. Chem. B* **1999**, *103*, 7367.
(51) Scaiano, J. C. *Handbook of Organic Photochemistry*; CRC Press: Florida, 1989.
(52) Berlman, I. B. *Handbook of Fluorescence Spectra of Aromatic Molecules*, 2nd ed.; Academic Press: New York, 1971.
(53) Perrin, D. D.; Armarego, W. L. F.; Perrin, D. R. *Purification of Laboratory Chemicals*, 2nd ed.; Pergamon: Oxford, 1980.

monitoring at the Raman band of a cell filled with demineralized water. The cells were painted black with camera varnish on two adjacent sides to avoid reflection at the quartz/air boundary. The decay traces were deconvoluted with a computer program[54,55] using nonlinear iterative least-squares fitting.

Cyclic Voltammetry. Cyclic voltammetry was performed using a BANK-Potentioscan model POS 73 with a Hewlett-Packard 7090A measurement/plotting system. Scan rates were 100−500 mV/s. Deoxygenated acetonitrile solutions were used (dried and stored on 4 Å molecular sieves) containing ca. 10^{-3} M of the compound studied and 0.1 M tetraethylammonium tetrafluoroborate (TEAB) as supporting electrolyte. A platinum disk working electrode and a platinum gauze auxiliary electrode were used, in combination with a saturated calomel reference electrode (SCE) connected to the sample solution via a 3 M KCl salt bridge.

Spectroelectrochemical Measurements. The UV−vis spectroelectrochemical measurements were carried out using a Perkin-Elmer Lambda 5 UV−vis spectrophotometer and an OTTLE cell[33] equipped with a Pt-minigrid working electrode (32 wires/cm) and quartz windows. The electrode potential was controlled during electrolysis by a PA4 potentiostat (EKOM, Czech Republic). Nitrogen-saturated butyronitrile solutions were used of the compound under study (10^{-3} M) with tetrabutylammonium hexafluorophosphate (TBAH) (3×10^{-1} M) as supporting electrolyte.

Transient Absorption Spectroscopy. Transient absorption spectra were measured with an EG&G OMA-III gated intensified diode array detector. The excitation source was a Lumonics XeCl excimer laser (308 nm, pulse width ∼ 7 ns). The pulse energy was attenuated to 1−10 mJ hitting the sample cell in a window 10 mm wide and 4 mm high. The probe light (right angle geometry) was a pulsed 450 W high-pressure xenon lamp, but the time window for observation was determined by gating the intensifier of the diode array. Timing of the pulses was accomplished using a digital delay generator (EG&G 9650). Spectra were averaged over up to 20 pulses for each delay to improve the signal-to-noise ratio. Commercially available spectrograde solvents were used. If the purity of the solvent was found to be insufficient, the solvent was purified by standard procedures.[53] Concentrations were adjusted to give $A_{1cm} \approx 1.0$ at 308 nm, and the samples were deoxygenated by purging with argon for 15 min.

(54) Spectrum Analyser: Kunst, A. G. M., University of Amsterdam, 1992.

(55) Fld Fit: Gedeck, P.; Jäger, W., University of Erlangen-Nürnberg, Germany, 1994.

The cosensitization experiments were carried out using a Q-switched Nd:YAG laser (355 nm, pulse width ca. 8 ns) as the excitation source. The radical cations were generated using 1,4-dicyanonaphthalene (DCN) as the photoexcitable acceptor and biphenyl ($E_{1/2}^{ox} = 1.96$ V vs SCE) as the cosensitizer. The concentrations were 10 mM DCN, 200 mM biphenyl, and <1 mM donor. The samples were made in acetonitrile and were not deoxygenated. The optical absorption at 355 nm was 1.0 cm^{-1}, entirely due to DCN.

Time-Resolved Microwave-Conductivity Measurements (TRMC). The TRMC measurements were carried out and analyzed as fully described elsewhere.[31,32] The excitation source was a Lumonics XeCl excimer laser (308 nm, pulse width ca. 7 ns, integrated intensity of approximately 10 mJ/cm^2 per pulse). Any transient change occurring after flash photolysis in the microwave conductivity (dielectric loss) was monitored as a change in microwave power reflected by the resonant cavity containing the solution of interest using a Tektronix 7912 transient digitizer. Concentrations were adjusted to give $A_{1cm} \approx 1.0$ at 308 nm, and the samples were deoxygenated by bubbling with CO_2 for 15 min.

Acknowledgment. The authors are grateful to H. J. van Ramesdonk and Ing. D. Bebelaar for their invaluable assistance with the photophysical experiments, to K. Goubitz and J. Fraanje for the determination of the crystal structure of **TC3**, and to G. W. H. Wurpel and E. Rienks for performing the Monte Carlo simulations on the specific solvation effects. This research was sponsored by the "Stichting Nationale Computer Faciliteiten" (National Computing Facilities Foundation, NCF) for the use of supercomputer facilities and supported (in part) by The Netherlands Foundation for Chemical Research (SON), with financial support from the Nederlandse Organisatie voor Wetenschappelijk Onderzoek (Netherlands Organization for Scientific Research, NWO).

Supporting Information Available: Descriptions of the synthetic methods used, details of the syntheses, and characterizations including the crystal structure determination (PDF). This material is available free of charge via the Internet at http://pubs.acs.org.

JA983716R